Binding Studies of Asymmetric Pentacoordinate Copper(II) Complexes Containing Phenanthroline and Ethane-1,2-diamine Ligands with Calf-Thymus DNA

by **Farukh Arjmand*** and **Mala Chauhan**

Department of Chemistry, Aligarh Muslim University, Aligarh 202002, Uttar Pradesh, India
(e-mail: farukh_arjmand@yahoo.co.in)

New chiral complexes of the composition [MLL′], where HL = 1,2-bis(1*H*-benzimidazol-2-yl)ethane-1,2-diol = H_2bimedol, M = Co^{II}, Ni^{II}, Cu^{II}, and L′ = 1,10-phenanthroline (phen) or ethane-1,2-diamine (en), were synthesized and characterized. The ligand L exhibited a coordination mode involving the O-atom of only one OH group, the other one being directed away from the metal center. The complexes [Cu(Hbimedol)(en)]Cl (**1**), [Cu(Hbimedol)(phen)]Cl (**2**), [Co(Hbimedol)(phen)]Cl (**3**), [Ni(Hbimedol)(en)]Cl (**4**), and [Ni(Hbimedol)(phen)]Cl (**5**) were ionic in nature and stable at room temperature. The donor sets involved in coordination with the metal ions were the O-atom of one OH group and two N-atoms of the two benzimidazole moieties, besides the two N-atoms of phen or en (*Fig. 1.*). The proposed five-coordinate geometry of **1**–**5** was established by analysis of spectroscopic data; the ball-and-stick models supported the proposed structures of **1**–**5** since they showed apparently no strain on any bond and angle. The interaction of complexes **1** and **2** with calf-thymus DNA were carried out by UV/VIS titration, circular dichroism, electrochemical methods, and viscometry. The intrinsic binding constant K_b of **1** and **2** was determined as $1.57 \cdot 10^4$ and $1.51 \cdot 10^4$ M^{-1}, respectively, suggesting that both complexes bind strongly to calf-thymus DNA.

Introduction. – Benzimidazole derivatives have been extensively studied as potential therapeutic agents [1–4] because the benzimidazole residue is a constituent of vitamin B_{12} [5], it shows pronounced biological properties [6–10], and has low cytotoxicity (IC_{50} values of 0.01–8 μg/ml) [11]. One of its derivatives, 1,2-bis(1*H*-benzimidazol-2-yl)ethane-1,2-diol (H_2bimedol; L) acts as chiral, facially coordinating tridentate ligand capable to modulate/direct the reactivity of the metal center. The introduction of such a chiral ligand with prospective donor O-atoms of OH groups and two imidazole N-atoms can afford stable pentacoordinate metal complexes in the presence of N,N donor ligands such as 1,10-phenanthroline or ethane-1,2-diamine. Synthesis of chiral transition-metal complexes by incorporating such a chiral auxiliary is a dynamic approach, which yields in an enantioselective manner robust complexes capable of selective binding to a molecular target site [12][13].

Cu Complexes are known to have a broad spectrum of biological action [14] as anti-inflammatory, antiarthritic, and antitumor agents [15]. It has been shown that the Cu accumulates in tumors due to selective permeability of the cancer cell membranes to Cu compounds; thus, a number of Cu complexes have been screened for anticancer activity, and some of them were found to be active *in vivo* and *in vitro* [16]. Five-coordinate Cu^{II} complexes are quite common, their configuration ranging from square pyramidal (*SP*) to trigonal-bipyramidal. The five-coordinated Cu^{II} complexes with an N,N donor heterocyclic base ligand have relatively better prospect in DNA binding

experiments [17]. Cu^{II} is an important *Lewis* acid center and an avid DNA-groove binder, and a heterocyclic base is amenable for functionalization for cellular use [18–20].

In this paper, we describe the synthesis and characterization of the chiral Cu^{II} complexes **1** and **2** (*Fig. 1,a*). We have also successfully synthesized the Ni^{II} and Co^{II} complexes **3**–**5** of the ligand H_2bimedol for structure elucidation. The binding of Cu complexes **1** and **2** with calf-thymus DNA (CT-DNA) was investigated by spectroscopic methods, viscosity measurements, and cyclic voltammetry. The results of the binding experiments were also supported by circular dichroism (CD) data.

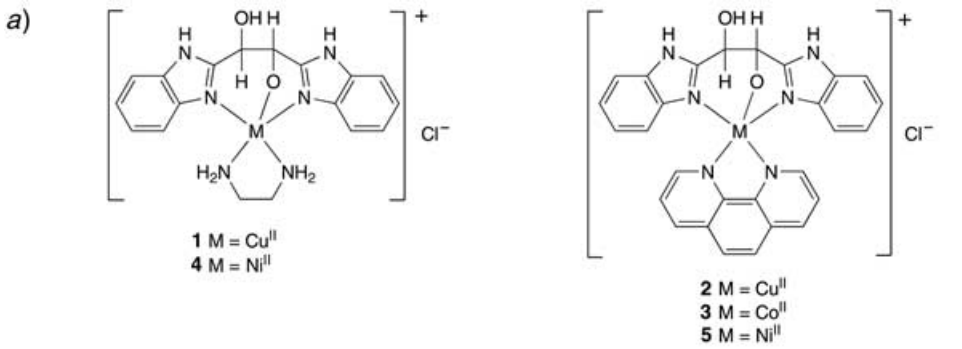

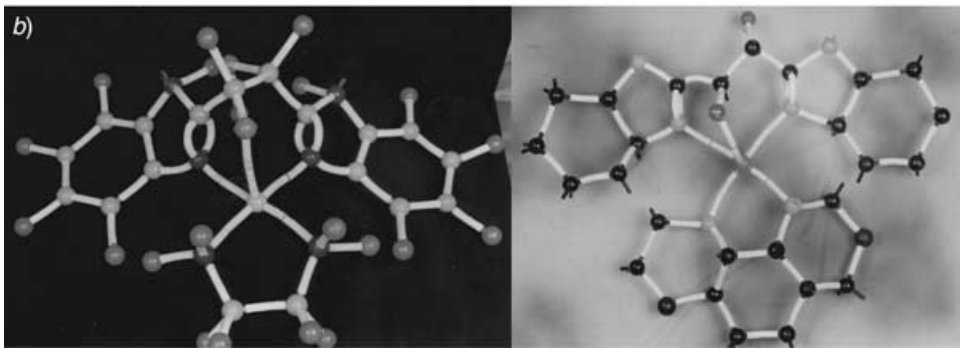

Fig. 1. a) *Chemical structures of complexes.* b) *Ball-and-stick models of complexes* **1** *and* **2**

Experimental. – *General*. Reagent-grade chemicals were used without further purification for all syntheses. $NiCl_2 \cdot 6\,H_2O$, $CuCl_2 \cdot 2\,H_2O$, ethylenediamine (*Merck*), $CoCl_2 \cdot 2\,H_2O$ (*BDH*), and 1,10 phenanthroline monohydrate (*CDH*) were used as received, and calf-thymus DNA (CT-DNA) was obtained from *Sigma*.

All the experiments involving interaction of the complexes with CT-DNA were performed in aerated buffer (0.01M, pH 7.5). Solns. of CT-DNA in buffer gave a ratio of UV absorbance at 260 and 280 nm of *ca.* 1.9 : 1, indicating that DNA was sufficiently free of protein [21]. The DNA concentration per nucleotide was determined by absorption spectroscopy with the molar absorption coefficient 6600 $dm^3\ mol^{-1}\ cm^{-1}$ at 260 nm. $[\alpha]_D$: *Rudolph Autopol III* polarimeter; MeOH solns. at 20°, 1-dm cell. Molar conductances: at r.t., *Digisun* electronic conductivity bridge. UV/VIS Spectra: *Ocean-Optics USB2000* spectrometer; MeOH solns., λ_{max} in nm. CD Spectra: *Jasco J-710-CD* spectropolarimeter; at 25° and 200–400 nm. IR Spectra: Nujol mull, *Interspec 2020* FTIR spectrometer; in cm^{-1}. ^{13}C- and ^1H-NMR Spectra: at 300 MHz; *Bruker DRX-300* spectrometer; δ in ppm. EPR Spectra: *Varian E-112* spectrometer; at the X-band frequency (9.1 GHz) at r.t. and liq.-N_2 temp. Microanalyses: *Carlo-Erba 1108* analyzer.

Cyclic Voltammetry (CV). All voltammetric experiments were performed with a *CH* electrochemical analyzer, in single compartmental cells at 25° with H_2O/MeOH 95:5 and 0.4M KNO_3 as a supporting electrolyte and a scan rate of $0.2\ Vs^{-1}$ in the potential range 1.6–1.2 V. A three-electrode configuration was used, comprised of a Pt microcylinder as the working electrode, a Pt wire as the auxiliary electrode, and an Ag/AgCl electrode as the reference electrode.

Viscosity Measurements. Ostwald's viscometer was used at $29 \pm 0.01°$, the flow time being measured with a digital stopwatch. Each sample was measured three times, and an average flow time was calculated. Data are presented as η/η_0 *vs.* the binding ratio [Cu]/[DNA], where η is the viscosity of DNA in the presence of complex and η_0 is the viscosity of DNA alone. Viscosity values were calculated from the observed flow time of DNA-containing solns. ($t > 100$ s) corrected for the flow time of buffer alone (t_0), $\eta = t - t_0$ [22]. The intrinsic binding constant K_b of the complex to CT-DNA was determined from *Eqn.* (*1*) [23] through a plot of $[DNA]/\varepsilon_a - \varepsilon_f$ *vs.* [DNA], where [DNA] represents the concentration of DNA, and ε_a, ε_f, and ε_b the apparent extinction coefficient (A_{obs}/[M]), the extinction coefficient for the free metal (M) complex, and the extinction coefficient for the free metal (M) complex in the fully bound form, respectively. In plots of $[DNA]/\varepsilon_a - \varepsilon_f$ *vs.* [DNA], K_b is given by the ratio of slope to intercept.

$$\frac{[DNA]}{\varepsilon_a - \varepsilon_f} = \frac{[DNA]}{\varepsilon_b - \varepsilon_f} + \frac{1}{K_b(\varepsilon_b - \varepsilon_f)} \quad (1)$$

*1,2-Bis(1*H*-benzimidazol-2-yl)ethane-1,2-diol* (*H_2bimedol*; L). The ligand L was prepared according to the procedure reported earlier [24]. ^{1}H-NMR (300 MHz, MeOH, 25°): 6.09 (OH); 7.10–7.45 (arom. H). ^{13}C-NMR (77.44 MHz): 154 (C=N; 129–134 (arom. C); 66.2 (CH).

*[1,2-Bis(1*H*-benzimidazol-2-yl-*κN^3*)ethane-1,2-diol-*κO^1*](ethane-1,2-diamine-*κN,κN$'$*)copper(1) Chloride* (*[Cu/Hbimedol)(en)]Cl*; **1**). To a soln. of $CuCl_2$ (1710 mg, 10 mmol) in MeOH (50 ml), ethane-1,2-diamine (0.67 ml, 10 mmol) was added slowly (→ blue soln.). Then H_2bimedol (2940 mg, 10 mmol) in EtOH (40 ml) and H_2O (10 ml) was dropwise under stirring at r.t. until complete dissolution. The resulting blue soln. was slowly evaporated. After 5 d, an amorphous green precipitate was obtained, washed thoroughly with hexane, filtered, and dried *in vacuo:* **1** (4 g, 75.2%). M.p. 240°. *Mmo*$_M$ (EtOH): 16.7 Ω^{-1} cm^2 mol^{-1} (1:1 electrolyte). $[\alpha]_D = +72$ (MeOH). UV/VIS (25°, $1 \cdot 10^{-4}$ M, EtOH): 265, 391, 589. IR (Nujol): 3497 (O–H), 1527 (C=N), 3180 (N–H), 1217 (C–O), 431 (M–O), 530 (M–N). Anal. calc. for $C_{18}H_{21}ClCuN_6O_2$: C 47.78, H 4.64, N 18.58; found: C 47.83, H 4.62, N 18.65.

*[1,2-Bis(1*H*-benzimidazol-2-yl-*κN^3*)ethane-1,2-diol-*κO^1*](1,10-phenanthroline-*κN$^{1'}$,κN^{10}*)copper(1) Chloride* (*[Cu(Hbimedol)(phen)]Cl*; **2**). As described for **1** with 1,10 phenanthroline (1980 mg, 10 mmol): **2** (5.3 g, 77.3%). M.p. 175°. *Mmo*$_M$ (EtOH): 26.1 Ω^{-1} cm^2 mol^{-1} (1:1 electrolyte). $[\alpha]_D = +108$ (MeOH). UV/VIS (25°, $1 \cdot 10^{-4}$ M, EtOH): 270, 325, 720. IR (Nujol): 3494 (O–H), 1529 (C=N), 3185 (N–H), 1213 (C–O), 430 (M–O), 532 (M–N). Anal. calc. for $C_{28}H_{21}ClCuN_6O_2$: C 58.74, H 3.67, N 14.68; found: C 58.56, H 3.62, N 14.74.

*[1,2-Bis(1*H*-benzimidazol-2-yl-*κN^3*)ethane-1,2-diol-*κO^1*](1,10-phenanthroline-*κN$^{1'}$,κN^{10}*)cobalt(1+) Chloride* (*[Co(Hbimedol)(phen)]Cl*; **3**). As described for **1** with $CoCl_2$ (2370 mg, 10 mmol) and 1,10-phenanthroline (1980 mg, 10 mmol): **3** (1.8 g, 25%). M.p. 240°. *Mmo*$_M$ (MeOH): 81.2 Ω^{-1} cm^2 mol^{-1} (1:1 electrolyte). $[\alpha]_D = +133$ (MeOH). UV/VIS (25°, $1 \cdot 10^{-4}$ M, EtOH): 256, 331, 505. IR (Nujol): 3494 (O–H), 1529 (C=N), 3185 (N–H), 1213 (C–O), 432 (M–O), 534 (M–N). Anal. calc. for $C_{28}H_{21}ClCoN_6O_2$: C 59.20, H 3.70, N 14.80; found: C 59.36, H 3.72, N 14.84%.

*[1,2-Bis(1*H*-benzimidazol-2-yl-*κN^3*)ethane-1,2-diol-*κO^1*](ethane-1,2-diamine-*κN,κN$'$*)nickel(1) Chloride* (*[Ni/Hbimedol)(en)]Cl*; **4**). As described for **1**, with $NiCl_2$ (2370 mg, 10 mmol) and ethane-1,2-diamine (0.67 ml, 10 mmol). The resulting deep blue soln. was treated with aq. NaOH soln. until pH 8–9 was reached (→ green soln.) and left at r.t. for slow evaporation. After 6 d, an amorphous light green precipitate was obtained, which was washed thoroughly with hexane, filtered, and dried *in vacuo:* **4** (4.0 g, 80.0%). M.p. 230°. *Mmo*$_M$ (MeOH): 85.0 Ω^{-1} cm^2 mol^{-1} (1:1 electrolyte). $[\alpha]_D = +33$ (MeOH). UV/VIS (25°, $1 \cdot 10^{-4}$ M, MeOH): 260, 390, 630. IR (Nujol): 3491 (O–H), 1527 (C=N), 3182 (N–H), 1213 (C–O), 428 (M–O), 531 (M–N). ^{1}H-NMR (300 MHz, MeOH, 25°): 12.34 (NH); 3.3 (CH_2); 6.01 (OH); 4.86 (CH); 7.18 (arom. H). ^{13}C-NMR (75.44 MHz): 156 (C=N); 134 (arom. C); 50.2 (CH). Anal. calc. for $C_{18}H_{21}ClN_6NiO_2$: C 48.30, H 4.69, N 18.78; found: C 48.45, H 4.72, N 18.84.

*[1,2-Bis(1*H*-benzimidazol-2-yl-*κN^3*)ethane-1,2-diol-*κO^1*](1,10-phenanthroline-*κN$^{1'}$$\kappa$N^{10}*)nickel(1) Chloride* (*[Ni(Hbimedol)(phen)]Cl*; **5**). As described for **4**, with 1,10-phenanthroline (1980 mg, 10 mmol) in place of ethane-1,2-diamine: **5** (5.0 g, 70.0%). M.p. 210°. *Mmo*$_M$ (MeOH): 83.2 Ω^{-1} cm^2 mol^{-1} (1:1 electrolyte). $[\alpha]_D =$

+384 (MeOH). UV/VIS (25°, $1 \cdot 10^{-4}$ M, MeOH): 257, 332, 600. IR (Nujol): 3491 (O–H), 1527 (C=N), 3182 (N–H), 1213 (C–O), 425 (M–O), 529 (M–N). ^{1}H-NMR (300 MHz, MeOH, 25°): 12.34 (NH); 7.12 (arom. H); 6.01 (OH); 4.86 (CH). ^{13}C-NMR (75.44 MHz): 156 (C=N); 134 (arom. C); 50.2 (CH). Anal. calc. for $C_{28}H_{21}ClN_6NiO_2$: C 59.23, H 3.70, N 14.80; found: C 58.35, H 3.76, N 14.82.

Results and Discussion. – *Syntheses.* The synthesis of the ligand H_2bimedol was a straightforward *Phillips* condensation reaction, and the complexes were prepared by the coordination of the ligands to the central metal ion *via* donor N- and O-atom. The N-atoms participate through coordinate linkages, while the O-atom is involved in coordination under release of HCl. The complexes conform to the composition [MLL′], where HL = H_2bimedol = 1,2-bis(1*H*-benzimidazol-2-yl)ethane-1,2-diol, M = Co^{II}, Ni^{II}, Cu^{II} and L′ = 1,10-phenanthroline or ethane-1,2-diamine as shown in *Fig. 1*, *a* and in the ball-and-stick model (*Fig. 1*, *b*). Evidently, the central metal ion acquires a square-pyramidal geometry in all the complexes. The complexes **1**–**5** are all soluble in EtOH and MeOH, but insoluble in H_2O, ionic in nature, and optically active, as also established by their CD spectra (see below).

IR Spectra. The IR spectra of the free ligand H_2bimedol display a characteristic $\tilde{\nu}$(O–H) band at 3497 cm^{-1} [25], a medium-intensity band at 1533 cm^{-1}, which is assigned to $\tilde{\nu}$(C=N) of the imidazole moiety [26], a characteristic $\tilde{\nu}$(N–H) stretching vibration at 3180 cm^{-1}, as well as $\tilde{\nu}$(C–N) and $\tilde{\nu}$(C–O) frequencies at 1317 and 1267 cm^{-1}, respectively. In the complexes **1**–**5**, the $\tilde{\nu}$(O–H) is replaced by a new absorption in the region 3478–3489 cm^{-1}, confirming the coordination of the metal ion through the O-atom of one of the OH groups of the ligand, while the other is uncoordinated. Furthermore, the $\tilde{\nu}$(C=N) of the imidazole moiety undergoes a negative shift of 8 cm^{-1}, indicating the involvement of N-atoms in the formation of the complexes. These data also support the contention that the ligand is tridentate with N,O,N donor sets. The far-IR spectra of **1**–**5** reveal $\tilde{\nu}$(M–O) and $\tilde{\nu}$(M–N) stretching vibrations in the range 430–450 and 535–580 cm^{-1}, respectively, confirming the square-pyramidal environment around the metal ions.

EPR Spectra. The solid-state X-band EPR spectra of **1** and **2** acquired at room temperature and liquid-N_2 temperature are anisotropic, exhibiting two peaks (*Fig. 2*). The EPR signals of **1** and **2** at room temperature with $g_\perp = 2.02–2.03$ and $g_\parallel = 1.97–1.98$ exhibit an inverse $g_\perp > g_\parallel \approx g_e$ pattern with unresolved hyperfine coupling, indicating a $\{d_{z^2}\}^1$ ground state for the complex, implying trigonal-bipyramidal geometry around the Cu^{II} ion [27]. This is inconsistent with the results of other spectral studies. Upon exposure to liquid-N_2 temperature, the EPR spectra of **1** and **2** reveal a large change in coordination geometry, as reflected by the '*g*' values $g_\parallel = 2.16–2.21$, $g_\perp = 2.02–2.06$, and $g_e = 2.0023$, which are different form the '*g*' values observed at room temperature. Since $g_\parallel > g_\perp \approx g_e$ is indicative of a $\{d_{x^2-y^2}\}^1$ or $\{d_{z^2}\}^1$ Cu^{II} ion, this pattern is consistent with a Cu^{II} ion in a distorted square-pyramidal geometry [28]. Such changes in EPR spectral features on changing the recording conditions, with variations in *g* values, suggest that the EPR spectra are crystal spectra rather than true molecular spectra [29].

NMR Spectra. The ^{1}H-NMR spectra (MeOH) of complexes **4** and **5** reveal that the characteristic signal at δ 6.09 [30] of the free OH groups of H_2bimedol disappears on complexation, suggesting that one OH group is coordinated to the metal center upon

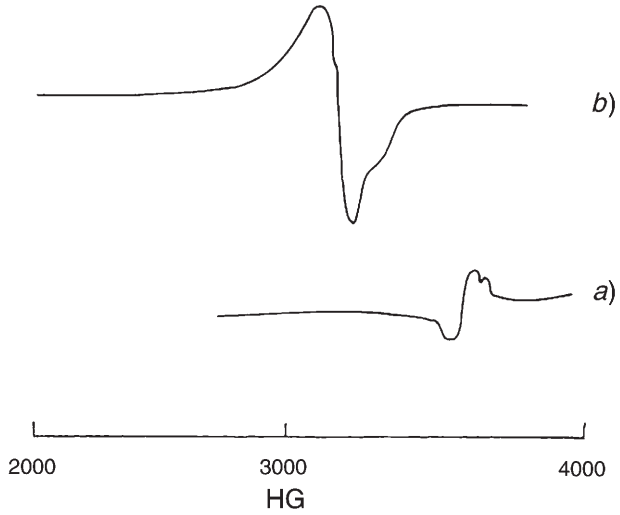

Fig. 2. *X-Band EPR spectra of complex* **2** a) *at room temperature and* b) *at liquid-N_2 temperature*

release of one HCl molecule. However, a new signal at δ 6.01 indicates that one of the OH groups is uncoordinated and involved in H-bonding with the anions and solvents. Also, the resonances of the NH, CH, and aromatic protons are slightly shifted in the spectra of the complexes as compared to those of the free ligand. The ^{13}C-NMR spectra confirm the ^{1}H-NMR data. The low-field δ(C) of C=N indicates the coordination of the N-atom to the metal center.

Electronic Spectra. The UV/VIS spectra (EtOH, 25°) for complexes **1** and **2** show a prominent broad band at 589 and 720 nm, respectively, ascribed to the d-d transition (d_{xz}, $d_{yz} \rightarrow d_{x^2-y^2}$), which are followed by strong bands in the UV region assigned to ligand-to-metal-charge-transfer (LMCT) transitions. These results are typical of square-pyramidal Cu^{II} complexes [31] with N-donors, which generally exhibit a single band between 585 to 750 nm (d_{xz}, $d_{yz} \rightarrow d_{x^2-y^2}$). In contrast, trigonal-bipyramidal Cu^{II} complexes usually show a maximum at >800 nm (d_{xy}, $d_{x^2-y^2} \rightarrow d_{z^2}$) with a higher-energy shoulder(d_{xz}, $d_{yz} \rightarrow d_{z^2}$) [31]. The bands at 589 (**1**) and 720 nm (**2**) thus confirm the square-pyramidal geometry of **1** and **2** as deduced by the EPR studies (liquid-N_2 temp.).

The UV/VIS spectra (EtOH) of **3** display a similar d-d transition at *ca*. 505 nm and strong bands in the UV region at 256 and 371 nm, consistent with a square-pyramidal environment of the Co^{II} ion [31].

The complexes **4** and **5** exhibit a d-d band at 600 and 630 nm assigned to the $^{3}B_1(F) \rightarrow {}^{3}E$ (F) and $^{3}B_1(F) \rightarrow {}^{3}A_2, {}^{3}E$ (P) transition, respectively [32]. The λ_{max} values are consistent with a pentacoordinate environment around the Ni^{II} ion . The spectra also show strong MLCT bands in the 320-nm region.

Electrochemistry. The cyclic voltammogram (MeOH/H_2O 5:95, 25°) of complex **1** in the absence of CT-DNA exhibits a quasireversible redox wave for a one-electron-transfer process, corresponding to a Cu^{II}/Cu^{I} redox couple with $E_{1/2} = -54$ mV and $\Delta E_p = 61$ mV (*Fig. 3,a*). The ΔE_p value is slightly larger than the *Nernstian* value

observed for a one-electron transfer couple. The large peak width for the one-electron couple $Cu^{II} \rightarrow Cu^{I}$ in **1** is a common observation [33]. This clearly indicates considerable reorganization of the coordination spheres during electron transfer regardless of the precise mechanism. The ratio of the anodic and cathodic peak currents I_{pa}/I_{pc} is *ca.* 1, implying a quasireversible electron transfer. At different scan rates, the voltammogram does not show any major change. Under the same recording conditions, the addition of CT-DNA ($c = 6 \cdot 10^{-3}$ M to **1** ($c = 0.1 \cdot 10^{-3}$ M) results in a shift in the $E_{1/2}$ and ΔE_p values (*Fig. 3,b*). The ratio I_{pa}/I_{pc} is 1.35 for the CT-DNA-bound complex **1** suggesting that the adsorption of the Cu^{I} product tends to be suppressed in the presence of CT-DNA [34]. Further, the shift in the $E_{1/2}$ and ΔE_p values with an increase in I_{pa}/I_{pc}values suggest that complex **1** is strongly bound to CT-DNA.

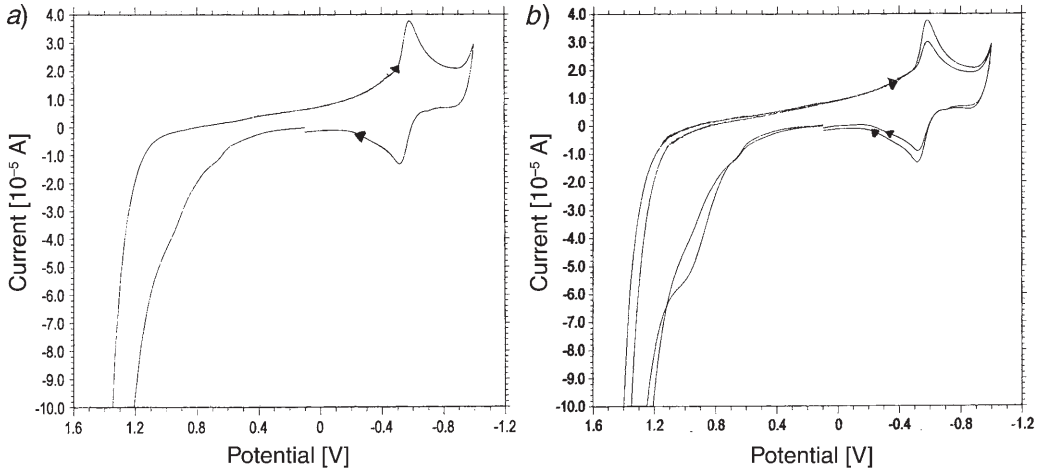

Fig. 3. *Cyclic voltammogram* (scan rate 0.2 Vs^{-1}, MeOH/H_2O 5:95, 25°) *of* a) *free complex* **1** *and* b) *complex* **1** *in the presence of CT-DNA*

The cyclic voltammogram MeOH/H_2O (5:95, 25°) of complex **2** ($c = 0.1 \cdot 10^{-3}$ M) reveals a one-electron quasireversible redox wave Cu^{II}/Cu^{I} with $E_{1/2} = -53$ mV and $\Delta E_p = 54$ mV (*Fig. 4,a*). The ratio I_{pa}/I_{pc} of *ca.* 1 suggests the reversibility of the process. On addition of CT-DNA to complex **2** as described above for **1**, the I_{pa}/I_{pc} ratio shifts to 0.684 (*Fig. 4,b*). The decrease in the I_{pa}/I_{pc} ratio in the presence of CT-DNA suggests that the adsorption of Cu^{I} is enhanced in the presence of CT-DNA. The decrease of I_{pa}/I_{pc} in case of **2** is in contrast to the increase I_{pa}/I_{pc} in case of **1**; however, both complexes **1** and **2** bind strongly to CT-DNA either by stabilization of the Cu^{II} over the Cu^{I} species or of the Cu^{I} species over the Cu^{II} species. Our interpretation is in fairly good agreement with the observation of *Mahadevan* and *Palaniandavar* [34].

The $E_{1/2}$ can be expressed as $E = E^0_{Cu^{II}-Cu^{I}} + 0.059 \log K(Cu)^{+}/K(Cu)^{2+}$. With $E = -0.104$ V (*vs.* NHE) and $E^0_{Cu^{II}-Cu^{I}} = -0.54$ and -0.53 V, we obtained the stability constant ratio $K(Cu)^{+}/K(Cu)^{2+} = 3.3 \cdot 10^{-7}$ and $1.6 \cdot 10^{-7}$ for complexes **1** and **2** in MeOH, respectively, which indicate that complex **1** is more stable than complex **2** [35].

Interaction Studies with CT-DNA. The UV/VIS absorption spectra of complexes **1** and **2** mainly consist of two resolved bands, the low-energy bands at 589 and 720 nm,

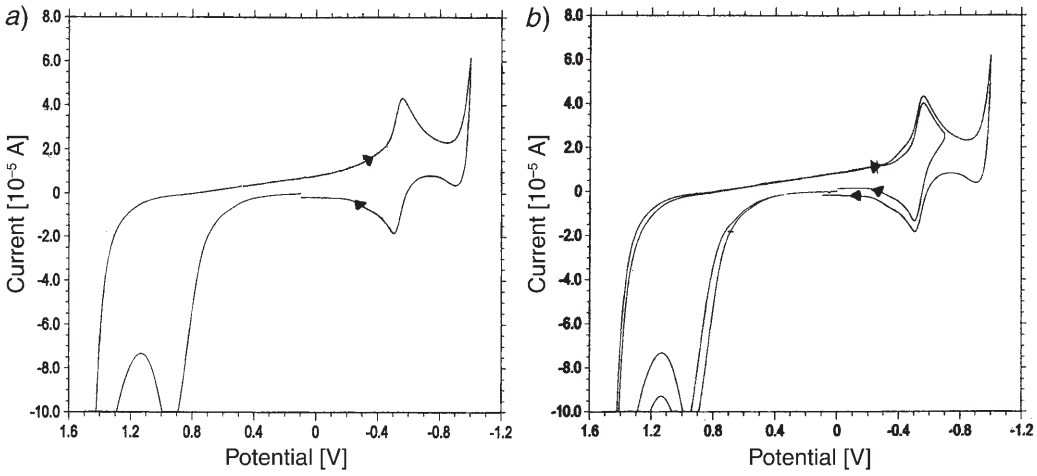

Fig. 4. *Cyclic voltammogram* (scan rate 0.2 Vs^{-1}, $MeOH/H_2O$ 5 : 95, 25°) *of* a) *free complex* **2** *and* b) *complex* **2** *in the presence of CT-DNA*

respectively, are assigned to the d-d transition (see above) and other bands at 232–276 nm, attributed to intraligand $\pi \rightarrow \pi^*$ transition. The interaction of complexes **1** and **2** with CT-DNA was investigated by titration of fixed amounts (0.83M) of the complexes with CT-DNA ($1.6-4.1 \cdot 10^{-5}$ M) and concomittant recording of the UV/VIS traces (*Fig. 5*). On addition of CT-DNA, the absorption spectra of these complexes exhibit hyperchromism [36] with a red shift of 2 and 4 nm, respectively, in intraligand transitions. The hyperchromic and hypochromic effect are the spectral features of DNA concerning its double-helix structure [37]. Hypochromism results from the contraction of DNA in the helix axis as well as from the change in DNA conformation, while hyperchromism results from the structural damage of DNA. Therefore, the observed hyperchromicities on addition of **1** or **2** to CT-DNA reflect strong structural damage, which is probably due to the strong binding of the complexes to the DNA base moieties through covalent-bond formation at the sixth vacant position of the coordination sphere of the metal ion. To study the binding affinity of **1** and **2** with CT-DNA, the intrinsic binding constants K_b of the complexes were determined with *Eqn. 1* [23] by monitoring the changes in absorbance of the intraligand bands with increasing concentration of CT-DNA. These intrinsic binding constants K_b of complexes **1** and **2** were thus determined to $1.57 \cdot 10^4$ and $1.51 \cdot 10^4$ M^{-1}, respectively [38]. The values indicate that both, **1** and **2**, moderately bind to CT-DNA with almost the same affinity. However, these values are smaller than those of classical intercalators and metallointercalators whose K_b values are in order of 10^7 M^{-1} [39]. Therefore, it is likely that the proposed covalent binding of the complexes **1** and **2** is more feasible although, in case of complex **2**, the 1,10-phenanthroline ligand may also be involved in π-π stacking in the DNA double-helix. Nevertheless, electrostatic interactions can not be ruled out.

Circular Dichroism. The CD spectrum (MeOH) of complex **1** at room temperature exhibits a strong positive *Cotton* effect around 254 nm (*Fig. 6,a*). On the other hand, complex **2** shows a positive rise at 287 nm and a negative band at 298 nm in the UV

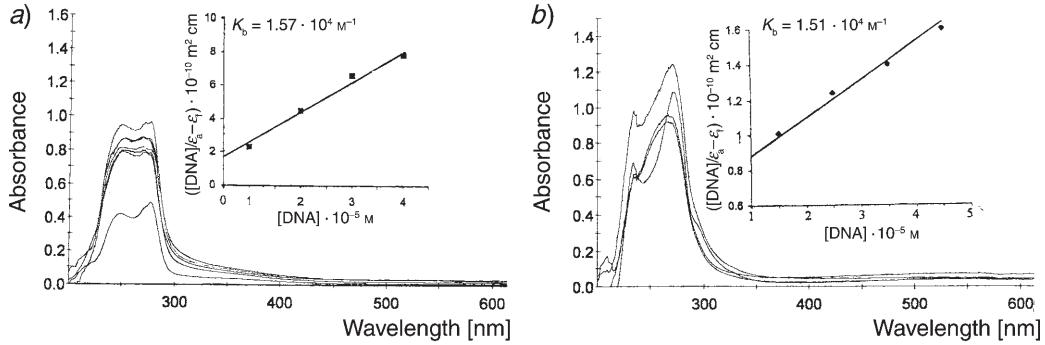

Fig. 5. *UV/VIS Spectra in* Tris · *HCl buffer of* a) *complex* **1** *and* b) *complex* **2** *upon addition of CT-DNA*. Inset: Plots of [DNA]/($\varepsilon_a - \varepsilon_f$) *vs.* [DNA] for the titration of CT-DNA with complexes; ■: experimental data points, solid lines: linear fit of the data.

region, as shown in *Fig. 6, b*, while in the VIS region, a strong positive *Cotton* effect is seen around 650 nm.

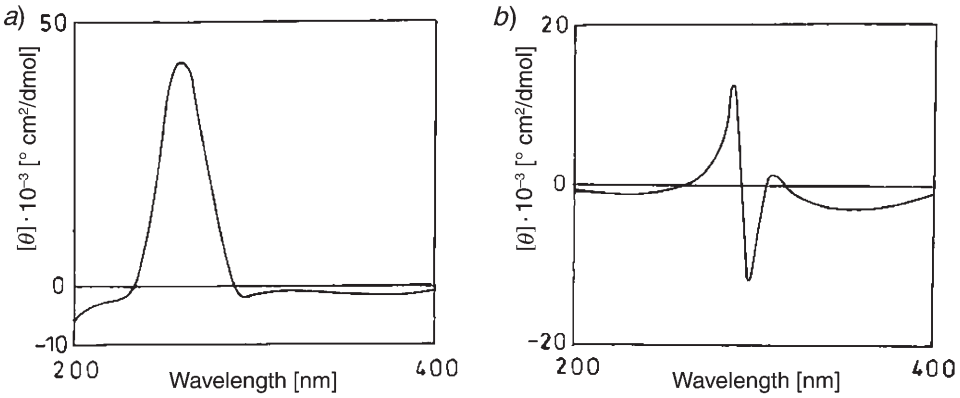

Fig. 6. *CD Spectra* (MeOH) *of* a) *complex* **1** *and* b) *complex* **2**

To study the binding behavior of **1** and **2** with CT-DNA, particularly the structural and conformational changes occurring in DNA on addition of these chiral complexes, the CD technique is extremely appropriate. The CD spectrum of CT-DNA in the UV region exhibits a positive band at 273 nm due to base stacking and a negative band 239 nm due to the helicity of DNA [34] (*Fig. 7, a*). Addition of complex **1** or **2** causes a significant and distinct spectral perturbation of the CD spectrum of CT-DNA. In the presence of **1**, the peak position shifts from 273 to 282 nm with an increase in positive ellipticity, while the intensity of the negative-ellipticity band decreases remarkably with no shift (*Fig. 7, b*). In the presence of **2**, a similar shift of the peak position as in the case of **1** occurs, but the intensity of both the positive- and negative-ellipticity bands decreases more (*Fig. 7, c*). These results support that a significant Cu^{II} complex – CT-DNA interaction takes place [40], and the binding of complexes with CT-DNA induces

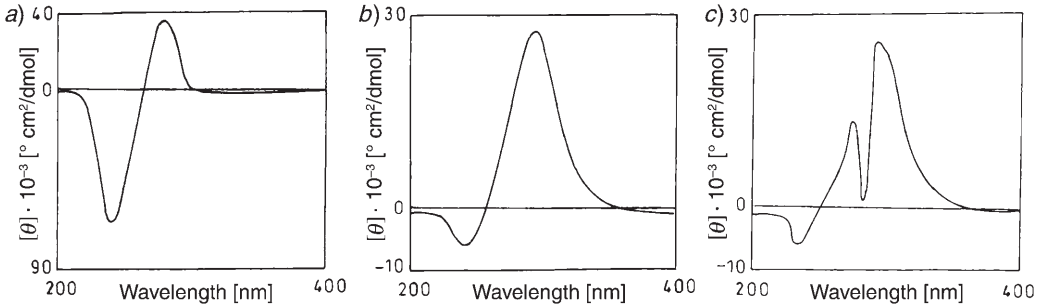

Fig. 7. *CD Spectra of* a) *CT-DNA alone,* b) *CT-DNA in the presence of complex* **1**, *and* c) *CT-DNA in the presence of complex* **2**. [DNA] = $3 \cdot 10^{-4}$ M.

conformational changes within the DNA molecule due to the *Lewis* acid nature of the Cu center [17].

Viscosity Studies. To support the binding model for the metal–DNA interaction, hydrodynamic viscosity measurements are quite useful, less ambiguous, and more accurate [41]. *Satyanarayana et al.* have elucidated vividly that in a classical intercalation model, the DNA helix lengthens as base pairs are separated to accommodate the bound ligand, leading to increased viscosity values of DNA. In contrast, a partial nonclassical intercalation of ligands causes a kink in the DNA helix and reduces the length and its viscosity [41][42]. The interaction of complex **1** or **2** with CT-DNA decreases the relative viscosity of CT-DNA with increasing concentration of the complex (*Fig. 8*). These results support that **1** and **2** bind to CT-DNA covalently [43].

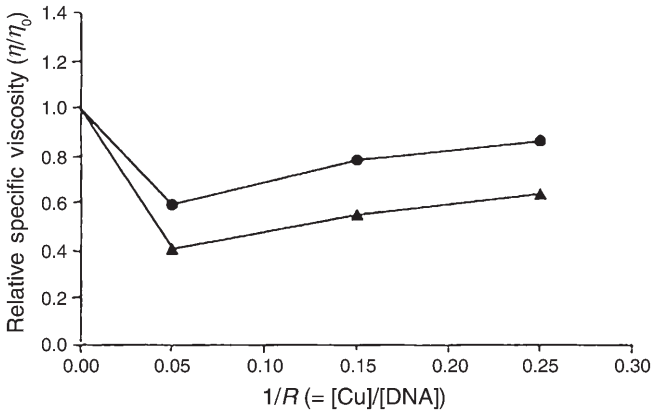

Fig. 8. *Effects of increasing amount of complex* **1** (●) *and complex* **2** (dov) *on the relative viscosity of CT-DNA at* $29 \pm 0.1°$. [DNA] = $5 \cdot 10^{-4}$ M.

We are grateful to the *University Grant Commission New Delhi*, India, for financial support through research grant No. F-12-21/2003 (SR). We thank the Regional Sophisticated Instrumentation Center, *C. D. R. I. Lucknow*, for supporting the C,H,N microanalysis, NMR spectra, and polarimetry, and *IIT*, Bombay, for EPR measurements. The authors gratefully acknowledge Dr. *S. Tabassum*, Aligarh Muslim University, and Dr. *R. P. Roy*, *N. I. I.*, New Delhi, for CD equipment.

REFERENCES

[1] N. H. Hauel, H. Nar, H. Priepke, U. Ries, J.-M. Stassen, W. Wienen, *J. Med. Chem*. **2002**, *45*, 1757.
[2] J. P. Lalezari, J. A. Aberg, L. H. Wang, M. B. Wire, R. Miner, W. Snowden, C. L. Talarico, S. Shaw, M. A. Jacobson, W. L. Drew, *Antimicrob. Agents Chemother*. **2002**, *46*, 2969.
[3] M. J. S. Moreno, A. F. Botello, R. B. G. Coca, R. Griesser, J. Ochock, A. Kotynski, J. N. Gutierrez, V. Moreno, H. Sigel, *Inorg. Chem*. **2004**, *43*, 1311.
[4] W. Andrada, I. A. Bagatin, A. M. Da Costa Ferreira, *Inorg. Chim. Acta* **2001**, *321*, 11.
[5] J. M. Pratt, in ' Handbook on Metalloproteins', Eds. I. Bertini, A. Sigel, H. Sigel, Marcel Dekker, Inc., New York, 2001, p. 603.
[6] A. W. White, R. Almassy, A. H. Calvert, N. J. Curtin, R. J. Griffin, Z. Hostomsky, K. Maegley, D. R. Newell, S. Srinivasan, B. T. Golding, *J. Med. Chem*. **2000**, *43*, 4084.
[7] D. J. Skalitzky, J. T. Marakovits, K. A. Maegley, A. Ekker, X.-H. Yu, Z. Hostmosky, S. E. Webber, B. W. Eastman, R. Almassy, J. Li, N. J. Curtin, D. R. Newell, A. H. Calvert, R. J. Griffin, B. T. Golding, *J. Med. Chem*. **2003**, *46*, 210.
[8] S. M. Sondhi, M. Johar, R. Shukla, R. Raghubir, N. Bharti, A. Azam, *Aust. J. Chem*. **2001**, *54*, 461.
[9] S. M. Sondhi, V. K. Sharma, N. Singhal, R. P. Verma, R. Shukla, R. Raghubir, M. P. Dubey, *Phosphorus, Sulfur Silicon Relat. Elem*. **2000**, *156*, 21.
[10] L. Benisvy, A. J. Blake, D. Collison, E. S. Davis, C. D. Garner, E. J. L. McInnes, J. McMaster, G. Whittaker, C. Wilson, *Chem. Commun.* **2001**, 1824.
[11] J. W. Lackey, D. S. Kinder, N. A. Tvermoes, to *Trimeris Inc.*, WO-02092575, 2002 (*IDrugs* **2003**, 6, 166).
[12] D. Fiedler, D. H. Leung, R. G. Bergman, K. N. Raymond, *J. Am. Chem. Soc.* **2004**, *126*, 3674.
[13] C. Sacht, M. S. Datt, S. Otto, A. Roodt, *J. Chem. Soc., Dalton Trans.* **2000**, 727.
[14] R. K. Crouch, T. W. Kensler, L. W. Oberlay, J. R. J. Sorenson, in 'Possible Medicinal Uses of Copper Chemistry', Eds. K. D. Karlin, J. W. Zubieta, Adenine Press, New York, 1986.
[15] D. Jayaraju, A. K. Kondapi, *Curr. Sci*. **2001**, *81*, 787.
[16] N. K. Singh, S. B. Singh, A. Srivastava, *Metal-Based Drugs* **2002**, *9*, 109.
[17] S. Dhar, P. A. N. Reddy, A. R. Chakravarty, *Dalton Trans.* **2004**, 697.
[18] A. Sreedhara, J. D. Freed, J. A. Cowan, *J. Am. Chem. Soc*. **2000**, *122*, 8814.
[19] T. Gajda, Y. Dupre, I. Torok, J. Harmer, A. Schweiger, J. Sander, D. Kuppert, K. Hegetschweiler, *Inorg. Chem*. **2001**, *40*, 4918.
[20] R. Ren, P. Yang, W. Zheng, Z. Hua, *Inorg. Chem*. **2000**, *39*, 5454.
[21] J. Marmur, *J. Mol. Biol.* **1961**, *3*, 208.
[22] M. Eriksson, M. Leijon, C. Hiort, B. Norden, A. Graslund, *Biochemistry* **1994**, *33,* 5031.
[23] A. Wolfe, G. H. Shimer, T. Meehan, *Biochemistry* **1987**, *26*, 6392.
[24] K. Isele, V. C. Broughton, J. Mattews, A. F. Willams, G. Bernardinelli, P. Franz, S. Decurtins, *J. Chem. Soc., Dalton Trans.* **2002**, 3899.
[25] Y. Xie, W. Bu, A. Sun-Chi. Chan, X. Xu, Q. Liu, Z. Zhang, J. Yu, Y. Fan, *Inorg. Chim. Acta*. **2000**, *310*, 257.
[26] S. M. Annigeri, A. D. Naik, U. B. Gangadharmath, V. K. Revankar, V. B. Mahale, *Transition Met. Chem*. **2002**, *27*, 316.
[27] N. K. Solanki, E. J. L. McInnes, D. Collison, C. A. Kilner, J. E. Davies, M. A. Halcrow, *J. Chem. Soc., Dalton Trans.* **2002**, 1625.
[28] M. Du, Y. M. Guo, X. H. Bu, J. Ribas, M. Monfort, *New J. Chem*. **2002**, *26*, 939.
[29] F. E. Mobbs, D. Collision, 'Electron Paramagnetic Resonance of d Transition Metal Compounds', Elsevier, Amsterdam, 1992, p. 73.
[30] K. M. Walters, M. A. Buntine, S. F. Lincoin, K. P. Waimwright, *J. Chem. Soc., Dalton Trans.* **2002**, 3571.
[31] K. Matsumoto, N. Sekine, K. Arimura, M. Ohba, H. Sakiyama, H. Okawa, *Bull. Chem. Soc. Jpn*. **2004**, *77*, 1343.
[32] M. D. Santana, G. Garcia, A. Rufete, M. C. R. Arellano, G. Lopez, *J. Chem. Soc., Dalton Trans.* **2000**, 619.
[33] A. J. Bard, L. R. Faulkner, 'Electrochemical Methods', Wiley, New York, 1980, p. 219.
[34] S. Mahadevan, M. Palaniandavar, *Inorg. Chem*. **1998**, *37*, 693.
[35] J. Casanova, G. Alzuet, J. Borras, O. Carugo, *J. Chem. Soc., Dalton Trans.* **1996**, 2239.
[36] C. Tu, Y. Shao, N. Gan, Q. Xu, Z. Guo, *Inorg. Chem*. **2004**, *43*, 4761.
[37] P. Yang, M. L. Guo, B. S. Yang, *Chin. Sci. Bull.* **1994**, *12*, 987.
[38] M. Baldini, M. B. Ferrari, F. Bisceglie, G. Pelosi, S. Pinelli, P. Tarascon, *Inorg. Chem.* **2003**, *42*, 2049.
[39] M. Cory, D. D. Mckee, J. Kagan, D. W. Hanry, J. A. Miller, *J. Am. Chem. Soc*. **1985**, *107*, 2528.

[40] S. Mahadevan, M. Palaniandavar, *Inorg. Chim. Acta* **1997**, *254*, 291.
[41] S. Satyanarayana, J. C. Dabrowiak , J. B. Chairs, *Biochemistry* **1993**, *32*, 2573.
[42] S. Satyanarayana, J. C. Dabrowiak, J. B. Chairs, *Biochemistry* **1992**, *31*, 9319.
[43] H. Xu, K.-C. Zheng, H. Deng, L.-J. Lin, Q.-L. Zhang, L.-N. Ji, *New J. Chem.* **2003**, *27*, 1255.

Received March 5, 2005